Experimental and Molecular Pathology 126 (2022) 104763

Contents lists available at ScienceDirect

Experimental and Molecular Pathology

journal homepage: www.elsevier.com/locate/yexmp

Antihyperglycemic activity of L-norvaline and L-arginine in high-fat diet and streptozotocin-treated male rats

Hayarpi Javrushyan [a], Edita Nadiryan [b], Anna Grigoryan [c], Nikolay Avtandilyan [a,b,*], Alina Maloyan [d]

[a] Research Institute of Biology, Yerevan State University, Armenia
[b] Department of Biochemistry, Microbiology and Biotechnology, Yerevan State University, Armenia
[c] Department of Human and Animal Physiology, Yerevan State University, Armenia
[d] Center for Developmental Health, Knight Cardiovascular Institute, Oregon Health & Science University, Portland, Oregon 97239, USA

ARTICLE INFO

Keywords:
Hyperglycemia
Dyslipidemia
Pre-diabetes
L-norvaline
Arginase
High fat diet
Nitric oxide
Streptozotocin

ABSTRACT

Background: A decrease in nitric oxide (NO) bioavailability has been shown to cause hyperglycemia, type II diabetes mellitus (DM), and chronic cardio-metabolic complications. In turn, hyperglycemia and hypercholesterolemia are associated with increased oxidative stress that leads to reduced nitric oxide bioavailability through disruption of L-arginine transport into cells, inactivation of nitric oxide synthase, and activation of arginase. Upregulation of arginase has been demonstrated in both diabetic patients and animal models of hyperglycemia and type 2 diabetes. L-norvaline is a nonselective inhibitor of arginase that increases NO production and promotes the normal functioning of the vascular endothelium. Another means of increasing NO bioavailability in the cardiovascular system is L-arginine supplementation. Whether L-norvaline and L-arginine have antihyperglycemic effects has not been studied.

Hypothesis: We hypothesized that inhibition of arginase will provide an antihyperglycemic effect and, as a result of the recovery of NO bioavailability, will protect against oxidative stress and hypercholesterolemia.

Methods: Rats were fed a high-fat diet (HFD) for three weeks concomitant with the two-time injection of 30 mg/kg of streptozotocin (STZ) to induce stable hyperglycemia. We studied the antihyperglycemic properties of arginase inhibition (via L-norvaline) and its combination with NOS substrate supplementation (via L-arginine).

Results: Treatment of HFD/STZ mice with L-norvaline and L-arginine reduced fasting blood glucose levels by 27.1% vs. untreated HFD/STZ rats ($p < 0.001$). Blood levels of total cholesterol, low-density lipoprotein (LDL), and malondialdehyde (MDA), a marker for oxidative stress, were significantly decreased in both L-norvaline- and L-norvaline+L-arginine-treated HFD/STZ rats when compared with untreated rats. In addition, administration of L-norvaline and L-arginine reversed the progression of pancreatic and kidney pathology in HFD/STZ rats as assessed by histology ($p < 0.001$).

Conclusions: Both L-norvaline and L-arginine act as potent antihyperglycemic agents and can represent alternative therapeutic tools in individuals with hyperglycemia and pre-diabetes.

Abbreviations: AGEs, Advanced glycation end products; BGL, blood glucose level; DM, Diabetes Mellitus; HFD, high-fat diet; HFD/STZ, high-fat diet-streptozotocin-induced rats; I.P., intraperitoneal; LDL, low density lipoprotein; MDA, malondialdehyde; NO, Nitric oxide; NOx, Stable NO products nitrate and nitrite; NOS, Nitric Oxide Synthase; eNOS, endothelial NOS; iNOS, inducible NOS; nNOS, neuronal NOS; N_{CLI}, number of cells of the islets of Langerhans; ox-LDL, oxidized low-density lipoproteins; PKC, Protein kinase C; ROS, Reactive oxygen species; S_{LI}, area of the islets of Langerhans; STZ, streptozotocin; STZ_LN, HFD/STZ rats treated with L-norvaline; STZ_LN_LA, HFD/STZ rats treated with + L-norvaline + L-arginine; SEM, Standard Error of Mean; T1DM, type 1 diabetes melitu; T2DM, type 2 diabetes mellitus; TBARS, Thiobarbituric acid reactive substances; TC, Total cholesterol.

* Corresponding author at: 1 Alex Manoogian, Yerevan, RA 0025, Armenia.
E-mail addresses: hg.javrushyan@ysu.am (H. Javrushyan), edita.nadiryan@ysumail.am (E. Nadiryan), annagrigoryan@ysu.am (A. Grigoryan), nv.avtandilyan@ysu.am (N. Avtandilyan), Maloyan@ohsu.edu (A. Maloyan).

https://doi.org/10.1016/j.yexmp.2022.104763
Received 11 November 2021; Received in revised form 5 March 2022; Accepted 4 April 2022
Available online 7 April 2022

1. Introduction

Nitric oxide (NO) is known to be a multifunctional signaling molecule involved in maintenance of metabolic and cardiovascular homeostasis (Chen et al., 2018). There is a general agreement that chronic hyperglycemia and diabetes mellitus (DM) lead to impairments in NO production and bioavailability (Assmann et al., 2016). However, where some studies have reported increased NO levels in diabetic patients and animal models of diabetes (Adela et al., 2015; Pitocco et al., 2010; Salama et al., 2022; Tuhin et al., 2017), others have reported the opposite (Ayub et al., 2011; Krause et al., 2012). NO bioavailability has also been described as reduced in animal models of hyperglycemia, hypercholesterolemia, and obesity (Bender et al., 2007; Hua and Malinski, 2019; Kim et al., 2008; Tatsch et al., 2012).

Importantly, coupled NO synthase (NOS) activity leads to generation of NO, but its uncoupling produces reactive oxygen species such as peroxynitrite ($ONOO^-$) and nitrogen dioxide ($\cdot NO_2$), which can potentiate inflammatory injury to various tissues (Tessari, 2015). Overproduction of peroxynitrite can in turn further depress NO bioavailability (Bender et al., 2007; Pitocco et al., 2010). An uncoupling mechanism for endothelial NOS (eNOS) kicks in when either levels of the cofactor tetrahydrobiopterin (BH_4) are low or the NO precursor L-arginine is unavailable, causing eNOS to producs superoxide ($O2^-$) instead of NO (Rafikov et al., 2011).

It has been suggested that NO acts as an antioxidant in vivo, specifically inhibiting proatherogenic lipid oxidation, as increasing NO bioactivity through L-arginine supplementation was found beneficial in hypercholesterolemic animals (Schirmer et al., 2012). In addition, L-arginine has demonstrated beneficial effects in atherosclerosis and disturbed shear stress (Napoli et al., 2006). LDL-cholesterol is an important negative regulator of endothelial NO synthase activity (Schirmer et al., 2012), and it appears that LDL can influence eNOS activity either indirectly by altering the cholesterol content of caveolae or directly by initiating a signaling cascade (Chikani et al., 2004). Indeed, all LDL subclasses have been shown to unfavorably shift the $(NO)/(ONOO^-)$ ratio to very low levels, imposing noxious effects such as elevated oxidative stress and a shortage of cytoprotective NO (Hua and Malinski, 2019).

Hyperglycemia is also suggested to promote chemical inactivation of NO, as monitoring of in vitro NO generation by purified recombinant bovine eNOS revealed glucose to cause a concentration-dependent attenuation of detectable NO (Brodsky et al., 2001; Petrie et al., 2018). T2DM and hyperglycemia are also reported to reduce the bioavailability of NO (Bonavida, 2015; Gilinsky et al., 2020). Interestingly, high glucose has been reported to increase eNOS protein expression, but ultimately decreases the release of NO (Hoshiyama et al., 2003). Reduced NO bioavailability leads to increased intracellular reactive oxygen species and enhanced arginase activity (Akın et al., 2020; Chen et al., 2018), and seems to be associated with L-arginine deficiency (Hoshiyama et al., 2003). Moreover, as a competitor for L-arginine, the enzyme arginase has emerged as a key factor in the regulation of NO production (Kövamees et al., 2016).

Several methods have been developed for increasing NO bioavailability, including supplementation with L-arginine, L-citrulline, and arginase inhibitors to increase substrate availability for NOS (Lundberg et al., 2015). Among arginase inhibitors, L-norvaline in particular has attracted interest for being nonselective; it has the effect of increasing endogenous stocks of L-arginine and also increasing production of NO, thereby promoting normal functioning of vessel endothelium (Ming et al., 2009; Steppan et al., 2013). Several studies in rats with stress-induced arterial hypertension have shown L-norvaline to protect the endothelium, reduce blood pressure, and induce diuresis (Gilinsky et al., 2020; Konovalova and Chernomortseva, 2019; Pokrovskiy et al., 2011; Polis et al., 2019). However, the effects of L-norvaline on blood lipid profile and oxidative stress in the setting of hyperglycemia and diabetes remain unclear.

In this work, we studied the antihyperglycemic and protective properties of L-norvaline and L-arginine and further assessed the role of increased NO and its potential beneficial effects using a rat model of hyperglycemia. For this model, a high-fat diet (HFD) was used to induce insulin resistance, with subsequent low-dose streptozotocin (STZ) injection to cause mild dysfunction in pancreatic β-cells without completely shutting down insulin secretion (Guo et al., 2018). This model closely mimics the natural development of T2DM from insulin resistance to β-cell dysfunction, as well as its metabolic features, and has been used to investigate both the mechanisms involved in T2DM and the efficacy of potential therapeutic agents (Furman, 2021; Zhang et al., 2008). Here, by supplementing hyperglycemic rats with L-norvaline or with L-norvaline and L-arginine, we were able to restore L-arginine metabolism to its natural levels. We did not use NO donors that rapidly turn into free radicals; rather, the supplements used here increased NO bioavailability and reduced levels of glucose and free radicals, thus protecting the diabetes-targeted tissues.

2. Materials and methods

2.1. Materials, drugs, and chemicals

Streptozotocin (STZ, CAS No.: 18883–66-4), L-norvaline (arginase inhibitor, CAS No.: 6600-40-4), L-arginine (CAS No.: 74–79-3), and malondialdehyde tetrabutylammonium salt (MDA, CAS No.: 100683–54-3) were purchased from Sigma Chemicals (USA).

2.2. Ethical approval and the rat model of HFD and STZ-induced hyperglycemia

Animal research was approved by the National Center of Bioethics at Yerevan State University and conducted according to handling guidelines outlined in the directive 2010/63/EU (2010/63/EU, 2010). Rats were housed in standard cages (3500 cm^2) in a ventilated room at 25 °C. Animals were kept in invariable environmental and nutritional conditions with a 12-h light/dark cycle and were provided either standard chow or a high-fat diet and water ad libitum. Body weights were recorded weekly. The study was conducted on 25 male Wistar rats (60 days old) weighing 90 ± 10 g. Rats were randomly assigned into five experimental groups with five animals/group (Fig. 1, a): Group I (Control) – untreated controls; Group II – control rats injected with saline (vehicle for L-norvaline and L-arginine) and 0.01 M citrate buffer (vehicle for STZ); Group III – rats treated with a HFD and STZ; Group IV – HFD/STZ rats treated with L-norvaline; and Group V – HFD/STZ rats treated with L-norvaline+L-arginine. To create a rat model of hyperglycemia, 70-day-old rats were fed a high-fat diet (chow diet +25% lard) for three weeks (see diet compositions in Table 1). This diet with 48% of calories sourced from fat, referred to as the Western diet, is commonly used to promote diet-induced obesity and, in conjunction with a low dose of STZ, to enhance diabetes-related phenotypes like insulin resistance and glucose intolerance (Hintze et al., 2018). Two weeks into the HFD regimen, the 84-day-old rats were intraperitoneally (IP) injected with 30 mg/kg of STZ dissolved in 0.5 mL 0.01 M citrate buffer (Furman, 2021; Zhang et al., 2008). The STZ treatment was also repeated on day 91 (the 3rd week of the HFD). L-norvaline (20 mg/kg/day dissolved in 0.5 mL saline for Group IV and 0.25 mL saline for Group V) was administered by IP injection, starting from day 56 (eight weeks) post-STZ (or vehicle) and continuing every third day for five weeks. For Group V, L-arginine (30 mg/kg/day dissolved in 0.25 mL of saline) was administered IP in combination with L-norvaline.

2.3. Blood glucose level

Blood glucose concentrations were determined every three days after STZ injection using a digital glucometer (FreeStyle Freedom Lite, Abbott, USA). Blood samples were obtained from tail veins following an

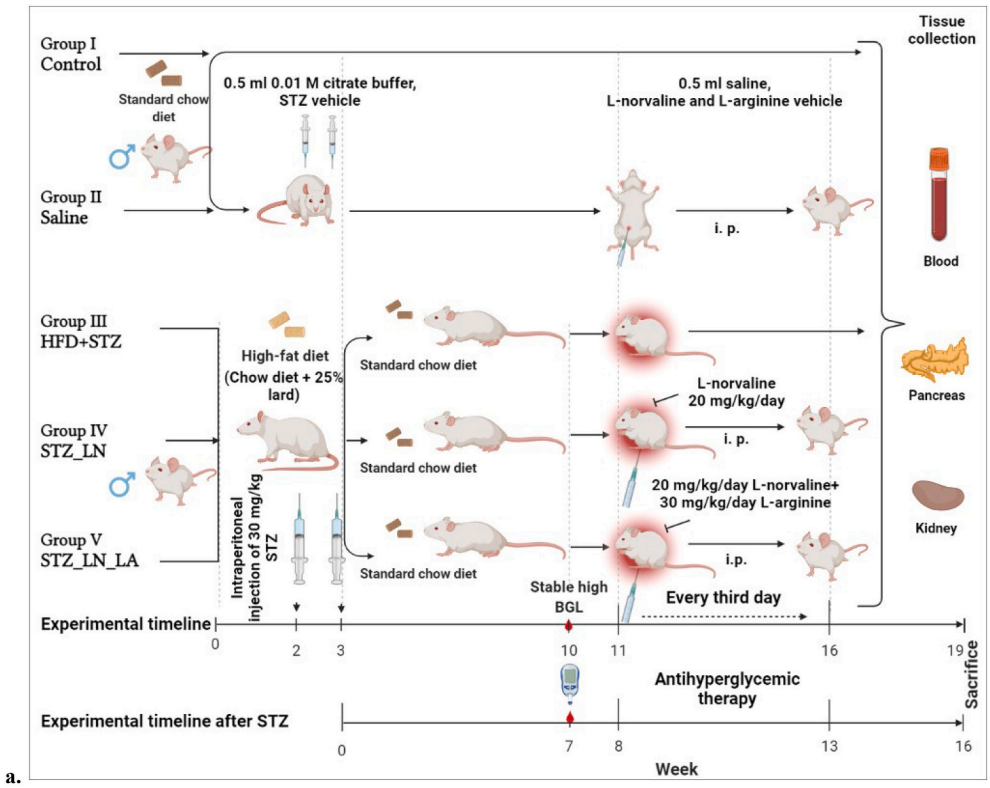

a.

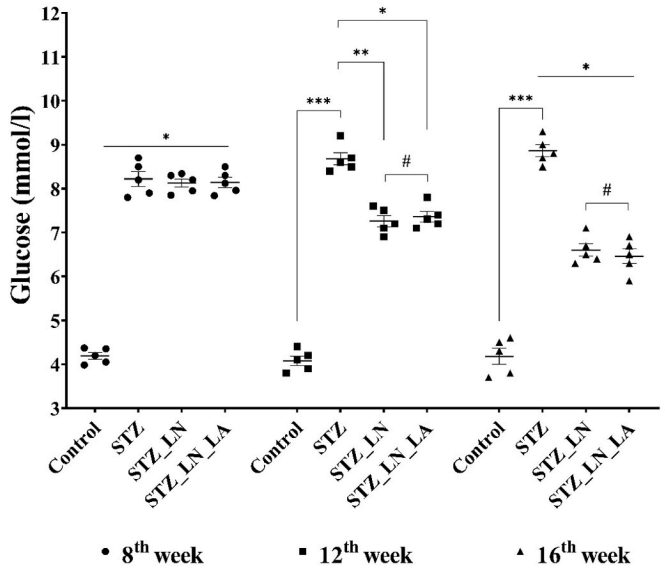

b.

Fig. 1. Experimental design (a) and blood glucose levels (mmol/L) in rats at selected timepoints after streptozotocin (STZ) administration (b). Rats were randomly assigned into five experimental groups with five animals/group: Group I (Control) – untreated controls; Group II – control rats injected with saline (vehicle for L-norvaline and L-arginine) and 0.01 M citrate buffer (vehicle for STZ); Group III – rats treated with a high-fat diet (HFD) and streptozotocin (HFD/STZ); Group IV – HFD/STZ rats treated with L-norvaline; and Group V – HFD/STZ rats treated with L-norvaline+L-arginine. To create a rat model of hyperglycemia, 70-day-old rats were fed a HFD (chow diet +25% lard) for three weeks. Two weeks into the HFD regimen, the 84-day-old rats were intraperitoneally (IP) injected with 30 mg/kg of STZ dissolved in 0.5 mL 0.01 M citrate buffer. The STZ treatment was also repeated on day 91 (the 3rd week of HFD). L-norvaline (20 mg/kg/day dissolved in 0.5 mL saline for Group IV and 0.25 mL saline for Group V) was administered by IP injection starting from day 56 (eight weeks) post-STZ (or vehicle) and continuing every third day for five weeks. L-arginine was administered IP (30 mg/kg/day dissolved in 0.25 mL of saline) in combination with L-norvaline. Dunn's comparison tests were non-significant among the Control, saline control, and citrate buffer control groups; accordingly, only results relative to the Control group are presented here. Data are represented as mean ± SEM. $N = 5$ animals/group. Statistical analysis across the experimental groups was performed using the Krustal-Wallis test and Dunn's multiple comparison test. Comparison of STZ_LN and STZ_LN_LA groups utilized the Mann-Whitney U test. * - $p < 0.05$, ** - $p < 0.01$, ***- $p < 0.001$. Quantitative glucose level is presented as of 8 (stable hyperglycemia), 12–13 (the end of treatment), and 16 (post-treatment period and end of the experiment) weeks after STZ administration. #, $p < 0.05$ STZ_LN vs. STZ_LN_LA.

overnight fast.

2.4. Measurement of NO content

NO levels were determined by measuring nitrite anions as described previously (Vodovotz, 1996). Briefly, 100 μL Griess reagent (0.2% naphthyl ethylenediamine dihydrochloride and 2% sulphanilamide in 5% phosphoric acid) was added to 100 μL of blood sample. The mixture was then added to tubes containing cadmium pellets, which convert nitrate to nitrite, and incubated at room temperature for 12 h. Absorbance was measured at 550 nm and normalized to a standard curve of $NaNO_2$.

2.5. Measurement of blood urea content

Arginase activity (kat, one mole of urea per second) in blood was determined by the diacetyl monoxime colorimetric method with modifications for blood (Avtandilyan et al., 2018).

2.6. Quantitative analysis of total cholesterol

Photometric determination of total cholesterol in serum was carried out using a modified Liebermann-Burchard reaction (Richmond, 1992). About 0.1 mL of blood serum was added to 2.1 mL of Ilke's reagent (50 mL of acetic anhydride, 10 mL of acetic acid, 10 mL of concentrated H_2SO_4). The samples were incubated at 37 °C for 20 min, after which

Table 1
Composition of standard chow and high-fat diet.

Macronutrients	Standard chow diet	High fat diet (+25% lard)
Crude protein %	20.2	20.2
Fat %	6.4	25.1
Carbohydrate (available) %	54.3	38.6
Neutral detergent fiber %	8.4	6.7
Crude fiber %	5.6	4.3
Minerals, vitamins, fatty acids, amino acids %	5.1	5.1
Energy density kcal/g	3.5	4.6
Calories from protein %	23	17
Calories from fat %	14	48
Calories from carbohydrate %	63	35

color intensity was measured by spectrophotometry at 630 nm.

2.7. Determination of low-density lipoprotein (LDL) in plasma lipoprotein fractions using a heparin-Ca precipitation technique

LDL quantity was determined by a previously-described method with minor modifications (March, 1989). A test tube was filled with 2 mL of $CaCl_2$ and 0.2 mL blood serum, then mixed gently. The optical density was determined at 630 nm in the absence (E1) or presence of heparin (0.04 mL, E2). Calculations utilized the following formula: LDL (mg/%) = (E2 - E1) x 1000.

2.8. Malondialdehyde (MDA) colorimetric assay

Lipid peroxidation was assayed by the thiobarbituric acid-malondialdehyde protocol (TBARS assay) with modifications following a previously-described method (Zeb and Ullah, 2016).

2.9. Histopathological examination of kidney and pancreas, and histological scoring

Pancreas and kidneys were fixed with 10% buffered formalin for 24 h. Tissues were then embedded in paraffin blocks, sectioned at approximately 5 μm thickness, and stained with hematoxylin and eosin (H&E) (Sigma-Aldrich, Taufkirchen, Germany). Stained sections were visualized by light microscopy (BM-190/T/SP Trinocular, Boeco, Germany), and representative images were captured using a CCD camera (B-CAM10, Boeco, Germany). Tissue sections were examined by a pathologist at the YSU Department of Human & Animal Physiology who was blinded to the experimental design. Histopathological alterations in the pancreas were graded according to the criteria of Spormann et al. (Spormann et al., 1989), which consider three aspects: acinar cell atrophy, vacuolization, and inflammatory cell infiltration, and were presented as histological scores. Histological scoring of pancreatic sections was performed to grade the extent of pancreatic parenchyma edema (0: no edema, 1: interlobular edema, 2: interlobular and moderate intralobular edema, 3: interlobular and severe intralobular edema), cell vacuolation (0: none, 1: 20% acini with vacuoles, 2: 50% acini, 3: >50% acini), and inflammation (0: no inflammation, 1: inflammatory cells present at intralobular, 3: inflammatory cells present at interacini). Histological scoring of kidney tissues was applied as described previously (Yen et al., 2012) in a blind fashion as well; the grading was based on loss of brush border, cast formation, and tubular dilatation, and binned into non-overlapping categories as follows: 0 (none), 1 (≤10%), 2 (11–25%), 3 (26–45%), 4 (46–75%), and 5 (≥76%). Average scores were calculated, and the final results expressed as mean ± SEM.

2.10. Histological assessment of pancreatic and renal tissue damage

The ratio of parenchyma and stroma cells (P/S) was calculated using stereological methods (Weibel et al., 1966). For each sample (each animal), exactly ten non-overlapping micrographs were taken over the entire surface of the tissue section at 100- and 400-fold magnification. Points corresponding with seminiferous tubules were evaluated as parenchyma tissue while all areas other than seminiferous tubules were accepted as stroma. The resulting images were processed using the Scopelmage 9.0 software (Maple, ON, Canada). Area values were determined for the islets of Langerhans, acinus, various elements of the stroma, and blood vessels of the pancreas and the kidneys. Additionally, the total number of cells in islets of Langerhans was counted, and the number of cells per unit area of the islets (N_{CLI}/S_{LI}) was calculated.

2.11. Statistics

Comparisons across groups were performed using Krustal-Wallis and Dunn's multiple comparison tests, and those between STZ_LN and STZ_LN_LA groups using the Mann-Whitney *U* test. Results are presented as mean ± SEM. Sample sizes for each experiment are shown in figure legends. A *p*-value of less than 0.05 was considered significant. Data were visualized using GraphPad Prism 9 software.

3. Results

3.1. Rat model of hyperglycemia

Seventy-day-old rats were fed either a regular or a high-fat diet (HFD consisting of a chow diet +25% lard for three weeks (Table 1). Two weeks into the HFD regimen, the rats were intraperitoneally (IP) injected with 30 mg/kg of STZ dissolved in 0.5 mL of 0.01 M citrate buffer (see Fig. 1, a for detailed groups description). The STZ treatment was repeated on day 91 (the 3rd week of HFD feeding). L-norvaline (20 mg/kg/day dissolved either in 0.5 mL saline for Group IV or in 0.25 mL saline for Group V) was administered by IP injection starting from day 56 (eight weeks) post-STZ (or vehicle) injection and continuing every third day for five weeks. For Group V, L-arginine was administered IP (30 mg/kg/day dissolved in 0.25 mL of saline) in combination with L-norvaline (Fig. 1, a). The outcomes of the experiments were analyzed at the following timepoints after STZ administration: week 8 (establishing stable hyperglycemia), weeks 12–13 (end of treatment), and week 16 (post-treatment period, end of the experiment). The following parameters were evaluated: blood glucose level (BGL), arginase activity, nitrite ions (e.g. NO), blood total cholesterol and LDL levels. Dunn's comparison tests were non-significant between the Control, saline control, and citrate buffer control groups; accordingly, only results related to the Control group are presented (Fig. 1, b). Stable hyperglycemia was observed starting from week seven after STZ injection. About 7–8 weeks after STZ administration, daily glucose measurements were consistently high, at 8.2 mmol/L in the STZ group vs. 4.2 mmol/L in the Control group ($p < 0.05$), indicating a hyperglycemic state.

3.2. Changes in blood glucose level (BGL)

As of week eight, fasting blood glucose levels (BGL) were increased by about 2-fold in the STZ, STZ_LN, and STZ_LN_LA groups relative to the Control group (8.22 mmol/L vs. 4.19 mmol/L, $p < 0.05$) (Fig. 1, b). At week 12, BGL in the HFD/STZ group was increased 2.1-fold (8.68 mmol/L) compared to the Control group (4.1 mmol/L) ($p < 0.001$). However, in the STZ-injected rats treated with both_LN and LN_LA, BGL was decreased by 20% relative to the untreated HFD/STZ group, reaching 7.35 and 7.15 mmol/L, respectively. At the end of the experiment (week 16), the STZ group was still exhibiting high BGL (8.84 mmol/L vs. 4.18 mmol/L for the Control group, $p < 0.001$). Meanwhile, in the STZ_LN and STZ_LN_LA groups, BGL continued to decrease, reaching a 26.1% reduction vs. the untreated HFD/STZ group (values of 6.7 and 6.5 mmol/L, respectively) ($p < 0.05$, Fig. 1, b). Importantly, no differences were observed between the LN and LN_LA treated groups, suggesting that LN was likely the main driver of the glucose-lowering

effect.

3.3. Changes in blood arginase activity and NO levels

Next, we studied the effect of L-norvaline and L-arginine on arginase activity and the abundance of nitrite ions (Fig. 2). We observed increased arginase activity on week eight post-HFD regimen plus STZ injection, with respective increases of 44.5%, 47.1%, and 48.3% in the STZ, STZ_LN, and STZ_LN_LA groups compared with the Control group ($p < 0.01$; Fig. 2, a). The effects of both LN and LN_LA treatments were evident in week 12, when excessive activation of arginase was reversed by 47.5% ($p < 0.01$). Importantly, the arginase activity in LN- and LN_LA-treated groups remained low at 16 weeks, indicating long-term efficacy of the treatments (Fig. 2, a). Again, no statistically significant differences in arginase activity were observed between the LN and LN_LA groups.

In addition, both treatments effectively prevented decrease in the levels of nitric oxide. As shown in Fig. 2b, the STZ group presented a progressive reduction in nitrite ion levels, being reduced by 26% and 30% in weeks 12 ($p < 0.05$) and 16 ($p < 0.01$), respectively, after STZ administration. However, treatment with LN ($p < 0.05$) and LN_LA ($p < 0.001$) increased levels of nitrite ions by 2- and 2.5-fold respectively vs. the HFD/STZ group, even reaching levels 35–45% higher than in the control group ($p < 0.05$). We also found that LN_LA treatment was more effective than treatment with LN alone ($p = 0.008$), indicating an additive effect of LA.

3.4. Changes in blood total cholesterol and LDL levels

Dyslipidemia is the major risk factor for cardiovascular diseases in hyperglycemic patients, and both hypercholesterolemia and increased LDL are key features of diabetic dyslipidemia (DiNicolantonio et al., 2016; Hirano, 2018). We next determined the effect of HFD and STZ on blood levels of LDL and total cholesterol. At eight weeks post-STZ treatment, blood LDL and cholesterol levels were increased 2.5-fold in the HFD/STZ group vs. Control ($p < 0.01$, Fig. 3, a and b). Those values remained high up to week 16 ($p < 0.01$, Fig. 3, a and b). At 12 weeks, both LN and LN_LA treatments reduced LDL levels by 53.7% and 66.8%, respectively, returning LDL concentrations to control levels by week 16 in the LN and LN_LA-treated groups (Fig. 3, a). Similarly, total cholesterol levels in the HFD/STZ group showed a gradual increase starting from week 8 of the experiment and continuing up to week 16 ($p < 0.01$),

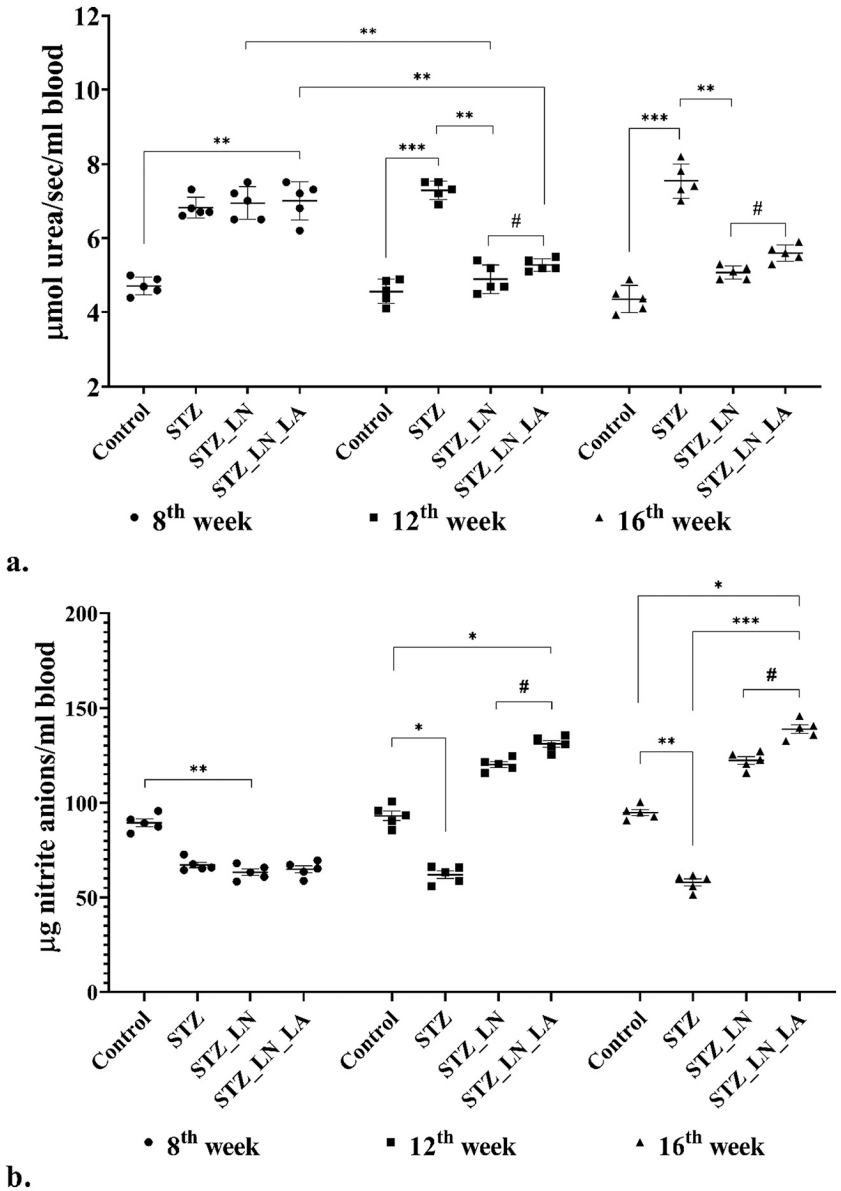

Fig. 2. Arginase activity (a) and nitrite anion content (b) in rat blood at selected time points after STZ administration: 8 (stable hyperglycemia), 12–13 (the end of treatment), and 16 (post-treatment) weeks. Data are represented as mean ± SEM. N = 5/group. Statistical analysis across experimental groups was performed using the Krustal-Wallis test and Dunn's multiple comparison test. Comparison of STZ_LN and STZ_LN_LA groups utilized the Mann-Whitney *U* test. * - $p < 0.05$, ** - $p < 0.01$, ***- $p < 0.001$; #, $p < 0.05$ STZ_LN vs. STZ_LN_LA.

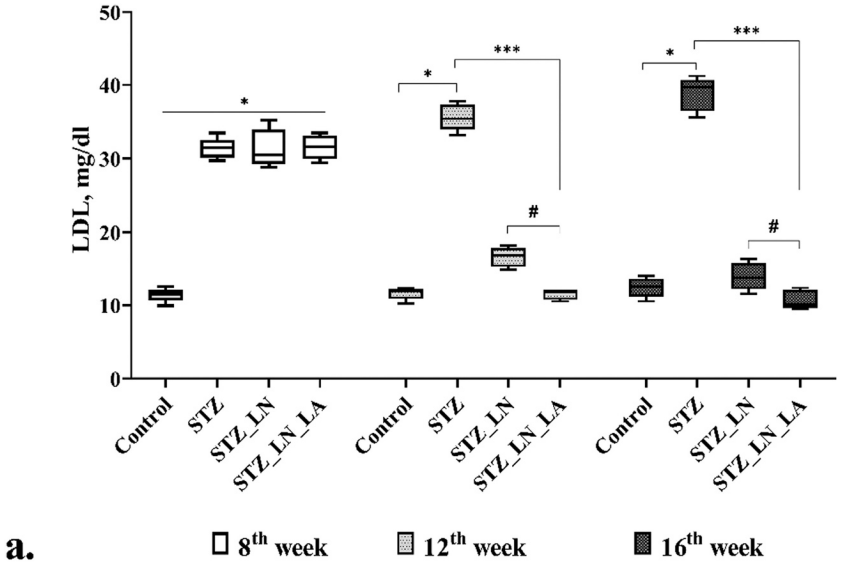

a.

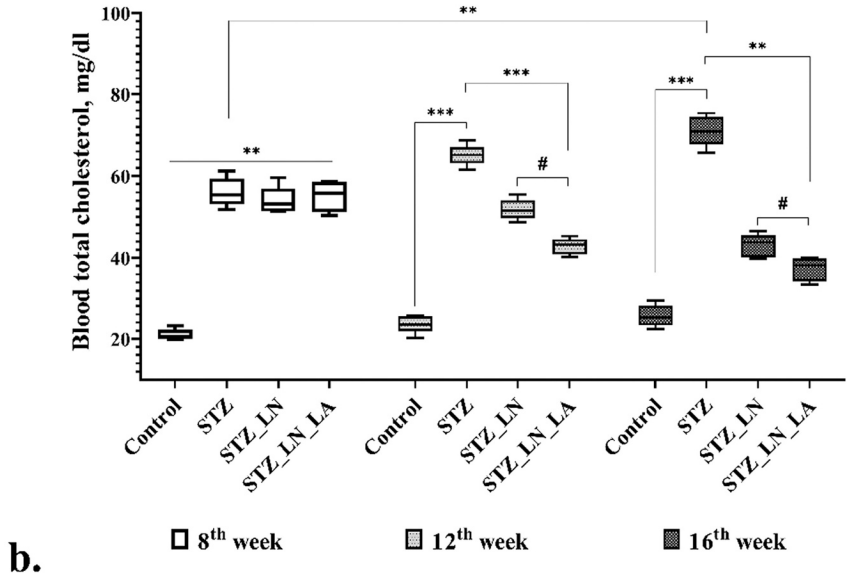

b.

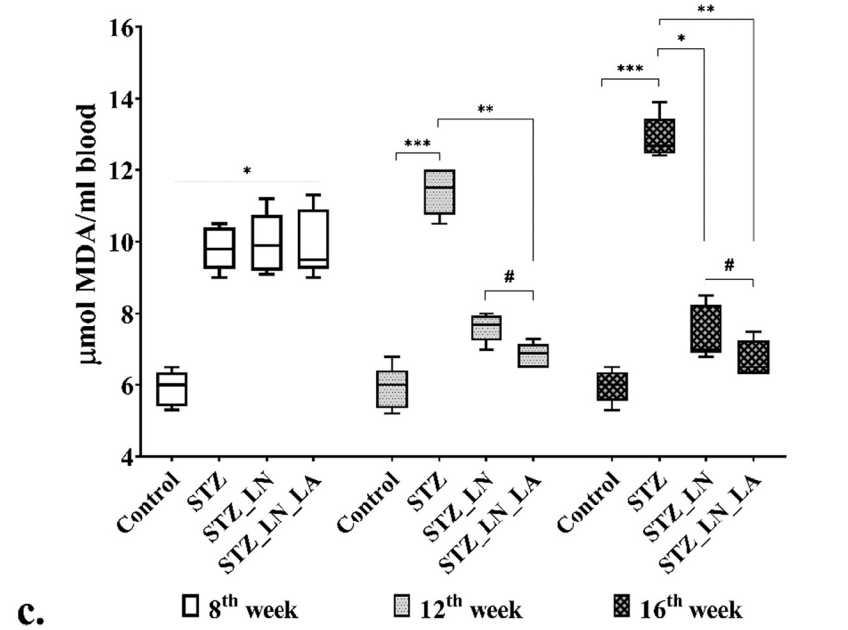

c.

Fig. 3. Blood lipid profiles in HFD/STZ-treated rats in the absence or presence of LN and LN_LA. LDL (a), total cholesterol (b), and MDA (c) were quantified in rat blood at 8, 12, and 16 weeks after STZ administration. Data are represented as mean ± SEM. $N = 5$. Comparisons of Control and STZ, STZ and STZ_LN, and STZ and STZ_LN_LA groups used the Kruskal-Wallis test and Dunn's multiple comparison test. Comparison of STZ_LN and STZ_LN_LA groups utilized the Mann-Whitney U test. * - $p < 0.05$, ** - $p < 0.01$, ***- $p < 0.001$; $^{\#}$, $p < 0.05$ STZ_LN vs. STZ_LN_LA.

while both LN and LN_LA treatments reduced cholesterol levels at 12 ($p < 0.001$) and 16 ($p < 0.01$) weeks vs. the untreated HFD/STZ group. Put specifically, at 12 weeks, cholesterol was decreased by 20.2% in the STZ_LN group and by 33.2% in the STZ_LN_LA group, and at 16 weeks by 38.9% in the STZ_LN group and 47.4% in the STZ_LN_LA group. Importantly, our data show that LN_LA treatment was more effective in reducing blood TC and LDL levels than LN treatment alone ($p < 0.05$, Fig. 3, a and b).

3.5. Changes in blood MDA levels

Hyperglycemia causes oxidative stress and excessive production of free radicals, leading to disruption of cellular functions, oxidative damage to membranes, and enhanced susceptibility to lipid peroxidation (Tangvarasittichai, 2015). Next, we measured the effect of HFD/STZ on oxidative stress in our model. Relative to Control rats, the hyperglycemic HFD/STZ rats exhibited elevated blood levels of malondialdehyde (MDA) throughout the entire experiment (Fig. 3, c). Importantly, STZ_LN and STZ_LN_LA groups showed a significant reduction in blood MDA levels vs. HFD/STZ rats at weeks 12 and 16 of the experiment ($p < 0.01$); moreover, the LN_LA treatment was more effective in reducing MDA levels than L-norvaline alone ($p < 0.05$). Both LN and LN_LA treatments also showed long-lasting effects, with MDA remaining low at 16 weeks despite the treatment having been completed by week 12 (Fig. 3, c).

3.6. Histological changes in the pancreas and kidney of HFD/STZ rats

To determine the effect of LN and LN_LA on pancreatic and kidney tissue damage caused by HFD and STZ, histological analyses were performed in all experimental groups. As stated in the Methods, a high histological score indicates profound pathological changes, while a low value indicates tissue morphology relatively more akin to normal. In the pancreas, histological analysis of the STZ group revealed decreases in the size and number of pancreatic islets (Fig. 4, b, black arrows). Meanwhile, the STZ_LN (Fig. 4, c and e, $p < 0.05$) and STZ_LN_LA (Fig. 4, d and e, $p < 0.01$) groups showed a significant preservation of islets in terms of both size and number (black arrows), indicating a beneficial effect of LN and LN_LA treatments. No differences were observed between LN and LN_LA treatments.

Kidney tissue sections stained with H&E likewise presented signs of epithelial damage in the HFD/STZ group (Fig. 5, b). The glomerular tuft area was shrunken with wrinkling of glomerular basement membranes, accompanied by a reduction of capillary lumen diameter (black arrows). Moreover, HFD/STZ rats showed significantly increased kidney histological score vs. Control rats ($p < 0.001$) (Fig. 5, a, b and e), indicating substantial histological abnormalities. Specifically, the cylindrical and cuboidal epithelium typical of healthy rats was absent, and vacuolation of epithelial cells and karyolysis were observed, features typical of diabetic kidneys. However, treatment with L-norvaline and L-arginine in combination restored renal cytoarchitecture, thereby reducing scores ($p < 0.05$) (Fig. 5, d and e). The Mann-Whitney test was non-significant when comparing STZ_LN and STZ_LN_LA (Fig. 5, e). All told, the adverse effects of HFD/STZ on kidney tissue were effectively prevented by four-week-long treatment with both LN and LN_LA.

3.7. The effect of L-norvaline and L-arginine on the relative areas of Langerhans islets and blood vessels of the pancreas and kidney

We next studied the effect of L-norvaline and L-arginine on the share of tissue area (%) occupied by Langerhans islets, components of the stroma, and blood vessels of the pancreas and kidney. Using light microscopy, we characterized 50 preparations of the pancreas and kidney, observing ten fields of view for each animal. We determined the percentages of the field of view respectively occupied by Langerhans islets, the various components of the stroma, the acinus, and blood vessels. The

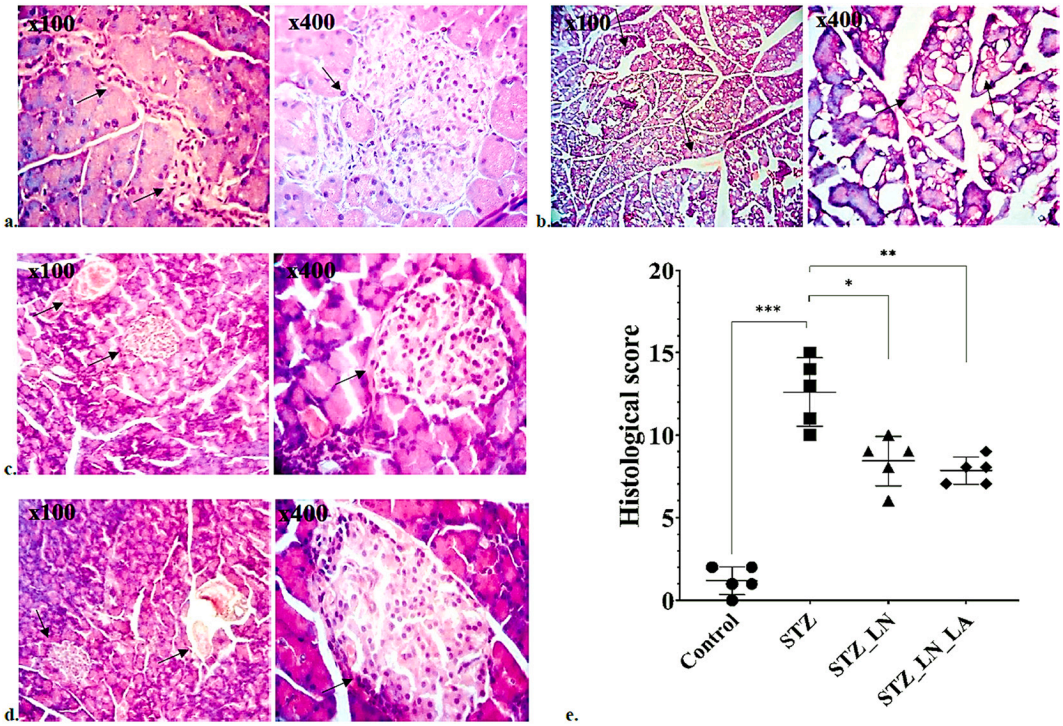

Fig. 4. Histopathological alterations in pancreatic tissue 16 weeks after STZ administration. Representative images (H&E staining, x100 and x400) for the Control group (a), HFD/STZ group (b), HFD/STZ + L-norvaline group (c), and HFD/STZ + L-norvaline+L-arginine group (d). Histological analysis was initially performed in a blinded fashion. Histological scores in the pancreas (e) were evaluated quantitatively based on three aspects: acinar cell atrophy, vacuolization, and inflammatory cell infiltration. HN = 5/group. Histological scores are presented as mean ± SEM. Comparisons of Control and STZ, STZ and STZ_LN, and STZ and STZ_LN_LA groups used the Krustal-Wallis test and Dunn's multiple comparison test. * - $p < 0.05$, ** - $p < 0.01$, ***- $p < 0.001$.

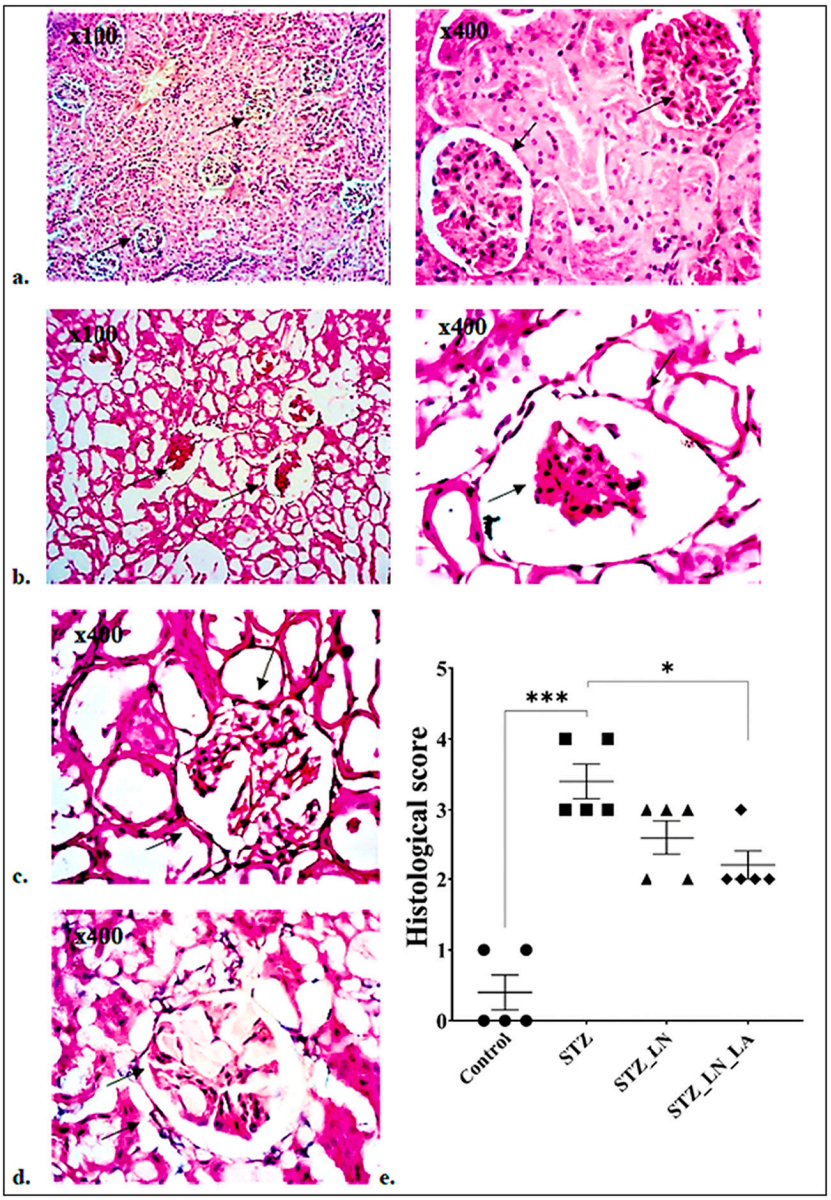

Fig. 5. Histopathological alteration in the kidney 16 weeks after STZ administration. Representative images (H&E staining, x100 and x400) for the Control group (a), HFD/STZ group (b), HFD/STZ + L-norvaline group (c), and HFD/STZ + L-norvaline+L-arginine group (d). Data are represented as mean ± SEM. N = 5/group. Comparisons of Control and STZ, STZ and STZ_LN, and STZ and STZ_LN_LA groups used the Krustal-Wallis test and Dunn's multiple comparison test. * - $p < 0.05$, ** - $p < 0.01$, ***- $p < 0.001$.

results are shown in Fig. 6. The HFD/STZ group presented a decrease in the areas taken up by islets ($p < 0.0001$) and blood vessels ($p < 0.05$) vs. the control group (Fig. 6, a). Meanwhile, the LN_ and LN_LA-treated groups exhibited greater percentages for islets of Langerhans ($p < 0.05$) and pancreatic blood vessels ($p < 0.0001$) than observed in the HFD/STZ group. These findings demonstrate the beneficial effects of LN and LN_LA in mice treated with HFD/STZ. Moreover, the islet area in the LN_LA group was greater than that in the LN group ($p = 0.033$) (Fig. 6, a). It is also noteworthy that the area occupied by pancreatic blood vessels in the HFD/STZ group was decreased 2.5-fold compared with the Control group, but blood vessel percentages in the LN and LN_LA groups were close to the values observed in the control group, with no statistically significant difference between LN and LN_LA. There were also no statistically significant differences between the LN and LN_LA groups regarding percent area of the pancreaetic acinus or stroma (Fig. 6, a).

When evaluating renal vasculature, we observed a 2-fold decrease in vascular surface area in the HFD/STZ group ($p < 0.001$) relative to the Control group (Fig. 6, b). Meanwhile, the LN and LN_LA treatment groups exhibited significantly improved renal blood vessel area ($p < 0.0001$), with values close to those of the Control group. No statistical difference was evident between LN and LN_LA treatments, suggesting that the two treatment models were similarly effective in preserving kidney vasculature.

We further quantified the ratio of islet cell number to islet area (Fig. 6, c) as the number of cells per 1 μm^2 and compared values between groups. A 3.5-fold decrease of islet cells was observed in HFD/STZ rats compared with Controls ($p < 0.0001$), while rats in the LN and LN-LA-treated groups exhibited 2 and 2.5 times more cells respectively than did the HFD/STZ group ($p < 0.0001$). Importantly, the LN_LA treatment was significantly more effective in this respect than LN treatment alone ($p = 0.03$) (Fig. 6, c).

4. Discussion

4.1. Overview of findings

Streptozotocin (STZ) is widely used to induce both insulin-dependent and insulin-independent diabetes mellitus by promoting β-cell death through DNA alkylation (Wu and Yan, 2015). While high doses of STZ mimic type 1 diabetes (T1DM) by severely impairing insulin secretion,

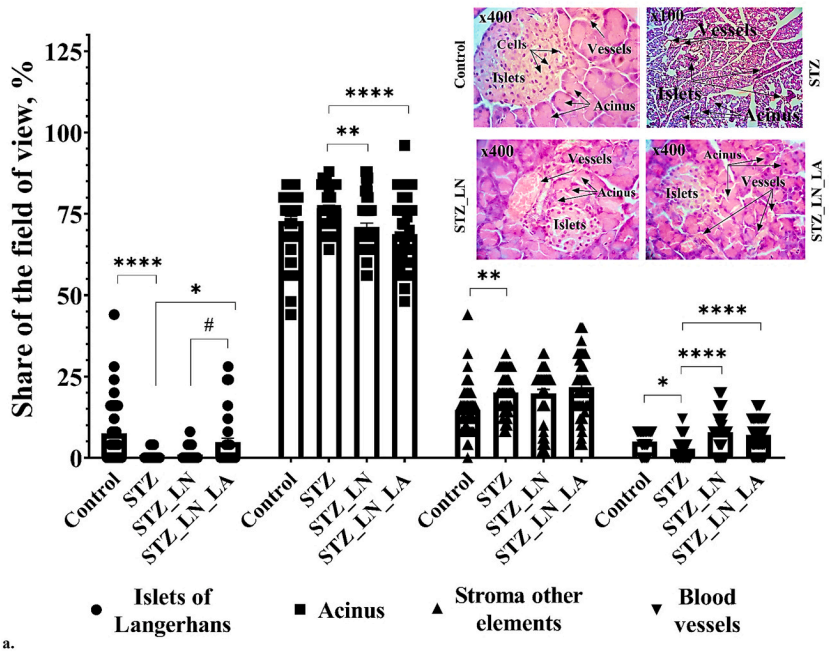

a.

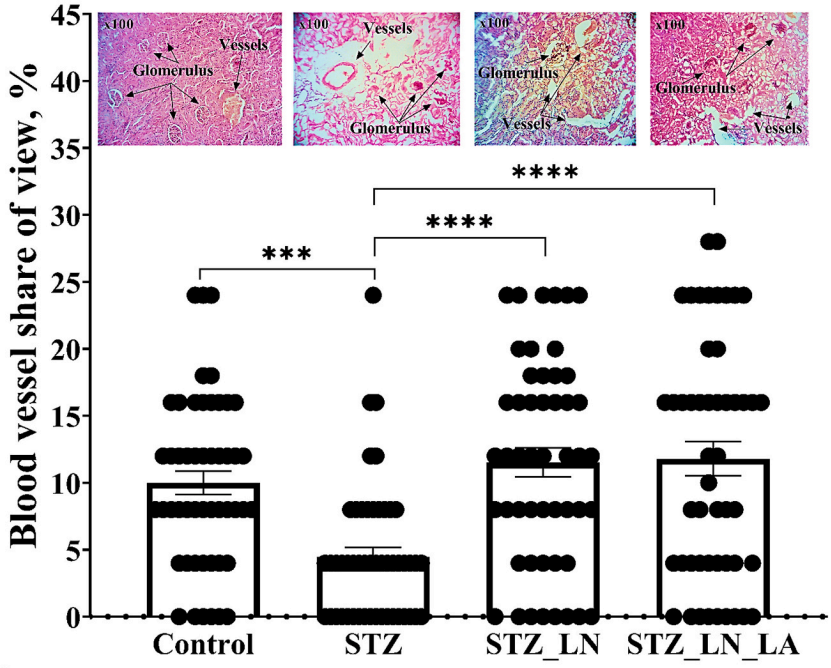

b.

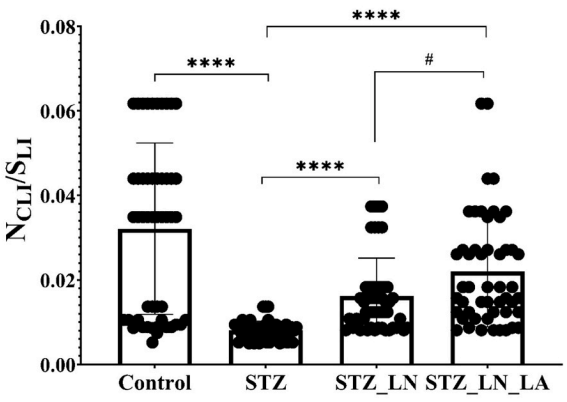

c.

Fig. 6. Quantification of pancreatic (a) and renal (b) tissue components (Langerhans islets, various components of the stroma, and blood vessels of the pancreas and kidney) and of total cells in Langerhans islets (c). Data are represented as mean ± SEM. N = 5/group. For each sample (each rat) ten non-overlapping micrographs were taken over the entire surface of the tissue section at 100- and 400-fold magnification. Comparisons of Control and STZ, STZ and STZ_LN, and STZ and STZ_LN_LA groups used the Krustal-Wallis test and Dunn's multiple comparison test. Comparison of STZ_LN and STZ_LN_LA groups utilized the Mann-Whitney U test. * - $p < 0.05$, ** - $p < 0.01$, ***- $p < 0.001$, ****- $p < 0.0001$; $^{\#}$, $p < 0.05$ STZ_LN vs. STZ_LN_LA. Abbreviations: N_{CLI} - number of cells in Langerhans islets, S_{LI} - area of Langerhans islets (μm^2).

low-dose STZ induces only mild impairment of insulin secretion, similar to features seen at later stages of type 2 diabetes. Therefore, investigators have developed a rat model in which feeding of a high-fat diet is followed by low-dose STZ injection, closely mimicking the natural progression of T2DM disease (Wu and Yan, 2015; Zhang et al., 2008). Many recent studies have employed this HFD/STZ-induced hyperglycemia model with a specific focus on understanding the beneficial effects of various synthetic and natural compounds on pancreatic ß-cells (Lertpatipanpong et al., 2021; Li et al., 2019). For example, studies were conducted to identify the regulatory and preventive effects of various signaling metabolic pathways in early and late diabetic complications (Al-Rasheed et al., 2016; Lee et al., 2021; Li et al., 2021; Xue et al., 2019). Our study was aimed at preventing hyperglycemic complications and protecting target tissues by modulating the L-arginine pathway. This study is the first to evaluate the antihyperglycemic, antioxidant, antidyslipidemic, and tissue damage preventive effects of L-norvaline and L-arginine (Fig. 7). Our results indicate that combined treatment with L-norvaline and L-arginine could provide a promising therapeutic tool for preventing adverse effects of hyperglycemia. The protective effects of L-arginine and L-norvaline stem from an increase in NO levels followed by reductions in fasting blood glucose, LDL, and total cholesterol; and furthermore in decreased lipid peroxidation and the prevention of pancreatic and kidney tissue damage otherwise seen in HFD/STZ rats (Fig. 7).

4.2. *Altered arginase activity and NO quantity in HFD/STZ-induced hyperglycemic rats*

Current data suggest that in the context of reduced NO bioavailability, upregulation of arginase is of central importance due to it competing with the endothelial form of NO synthase for the substrate L-arginine (Pernow and Jung, 2013). Plasma arginase activity is increased in type 2 diabetic patients with impaired NOS activity, and correlates with the degree of hyperglycemia (Kashyap et al., 2008). Altered serum NO in T1DM or T2DM patients has been reported by several studies, however results across the literature are controversial: some studies reported increased NO levels in diabetic patients, whereas others reported the opposite (Assmann et al., 2016; Krause et al., 2012). NO bioavailability has also been described as decreased in animal models of obesity and DM (Bender et al., 2007; Tatsch et al., 2012). In the present study, HFD/STZ-induced hyperglycemic rats exhibited reduced NO quantity and increased arginase activity in the serum when compared to the control group, which is in agreement with some previous reports (Assmann et al., 2016; Krause et al., 2012). The therapeutic model we offer has a rapid and long-term regulatory effect on arginase and NOS activity. Its effectiveness is due not to a decrease in glucose level (which remained at least 6.5 mmol/L), but rather to upregulation of NO. Notably, higher levels of NO are associated with higher glucose levels in diabetic patients both with and without coronary artery disease. Moreover, in *vitro studies* and animal models have confirmed that high serum glucose levels are responsible for the enhanced nitric oxide levels observed in cells. That said, it is not yet clear whether higher nitric oxide levels are beneficial or detrimental during the progression of diabetes. Possibly, elevated NO is part of the adaptation to high glucose concentrations (Adela et al., 2015). Here, we found combined supplementation with L-arginine and an arginase inhibitor to increase NO bioavailability, reduce production of reactive species, and ameliorate the inflammatory state of the pancreas. We

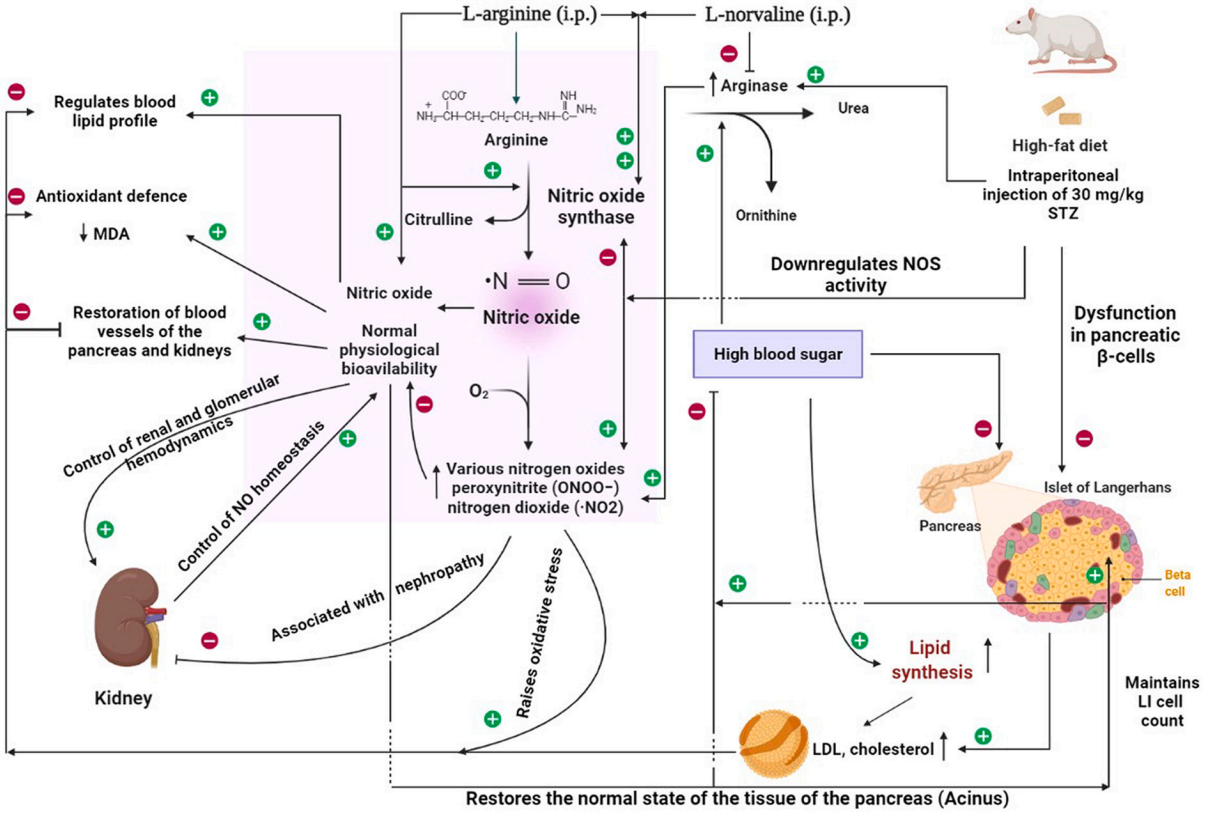

Fig. 7. Schematic of the beneficial effects of L-norvaline and L-arginine. Consumption of a high-fat diet (HFD) followed by low-dose streptozotocin (STZ) injection causes mild dysfunction in pancreatic β-cells and subsequent hyperglycemia. Our study suggests that combined treatment with L-norvaline and L-arginine could provide a promising therapeutic tool to prevent changes caused by hyperglycemia. The protective effects of this supplementation are rooted in an increase of NO levels followed by reductions in blood glucose, total cholesterol, and LDL; decreased lipid peroxidation; and prevention of histopathological changes in the pancreas and kidney. Abbreviations: MDA - malondialdehyde, LDL - low density lipoprotein, STZ - streptozotocin, i.p. – intraperitoneal, LI - islets of Langerhans. Created in part with BioRender.

hypothesize that the observed regulation of glucose levels in supplemented groups is not direct, as NO has an inhibitory effect on glycolysis (Muronetz et al., 2021), but rather indirect, through NO acting as an antioxidant and anti-hypercholesterolemic agent and via its protective effects on the pancreas.

4.3. Total cholesterol- and LDL-lowering activity of NO

Hyperglycemia is associated with multiple metabolic dysregulations, among which lipid metabolism is known to be affected by high concentrations of triglycerides, high levels of total cholesterol, and low levels of high-density lipoprotein (Galicia-Garcia et al., 2020; Schofield et al., 2016). Several previous reports have demonstrated anti-atherosclerotic effects of NO, achieved through its regulation of both exogenous and endogenous NOS (eNOS) activity (Gori, 2020; Huang et al., 2020). In contrast, inhibition of NOS has been shown to stimulate the development of atherosclerosis (Aluko et al., 2018); moreover, oxidized LDL triggers atherosclerosis by affecting eNOS activity and uncoupling, reducing the bioavailability of NO (Chen et al., 2018). Meanwhile, eNOS also plays a major role in the response to anti-hypercholesterol statin drugs. In a study of Jordanian T2DM patients, a significant association was observed between genotypes of two NOS single nucleotide polymorphisms, rs1799983 and rs61722009, and baseline levels of total cholesterol and LDL. These genetic variants thus affect cholesterol levels and play roles in susceptibility to cardiovascular diseases among T2DM patients (Abdullah et al., 2020). Previous reports have demonstrated that L-arginine supplementation restores NO levels via stimulation of nitric oxide biosynthesis and reduces vascular oxidative damage in hypercholesterolemic conditions (Harisa et al., 2016). It is logical to combine L-arginine supplementation and the arginase inhibitor L-norvaline for greater efficiency; investigation of the protective properties of L-norvaline against atherosclerosis is also underway in our laboratory.

In our study, HFD/STZ rats showed increased levels of LDL and total cholesterol. Meanwhile, treatment with L-norvaline or L-norvaline and L-arginine restored blood lipids to control levels. These results may be associated with the elevation of NO quantity. For one, nitric oxide regulates critical lipid membrane and lipoprotein oxidation events by contributing to the formation of potent oxidants; it also exhibits antioxidant properties, being able to terminate propagating lipid radicals and inhibit lipoxygenases (Förstermann et al., 2017; O'Donnell and Freeman, 2001). It is also possible that NO regulates lipogenesis, derived from the action of NO on coenzyme A (CoA) to produce metabolically inactive S-nitrosoCoA. As a third possibility, the beneficial effects of these treatments may be attributable to low activity of cholesterol biosynthetic enzymes under the control of NO (Förstermann et al., 2017). In addition, NO significantly impairs long-chain fatty acid and cholesterol synthesis in the liver (Roediger et al., 2004). It has been established that inadequate supply of cholesterol to the plasma membrane and lysosomes can result in insulin resistance and impaired autophagy (Seneff et al., 2012); restoring cholesterol levels to normal in turn restores the insulin sensitivity of the tissue. Thus, arginase inhibition and regulation of glucose and lipid metabolism may improve β-cell metabolism, thereby increasing insulin secretion and normalizing lipolysis and lipogenesis.

4.4. Antioxidant activity of arginase inhibition and increased NO

A high level of arginase activity is associated with increased oxidative stress, further impairing NO bioavailability (Pernow and Jung, 2013). Chronic hyperglycemia has a destructive influence on pancreatic β-cells through inducing oxidative stress, which is more problematic than in other cells because β-cells possess the lowest intrinsic antioxidant defenses. Glucose possibly increases ROS formation through the non-enzymatic glycation of proteins, as well as through auto-oxidation (Gerber and Rutter, 2017). Hyperglycemia stimulates the production of advanced glycation end products (AGEs) and enhances the polyol, protein kinase C (PKC), and hexosamine pathways, which may lead to oxidative stress (Assmann et al., 2016; Pitocco et al., 2010). In our study, a significant increase in MDA level was observed in the serum of HFD/STZ-induced hyperglycemic rats; however, treatment with L-norvaline or the combination of L-norvaline and L-arginine lowered MDA to near-normal levels. In light of the literature and the results we have obtained, we conclude that the MDA reduction could be explained by reductions in blood glucose level and arginase activity.

4.5. The protective effect of L-norvaline and L-arginine on hyperglycemia-induced tissue damage

H&E staining of pancreas and kidney tissues derived from STZ-hyperglycemic rats indicated significantly increased histological scores compared with control healthy rats (Fig. 4, e and Fig. 5, e). The histopathological findings in this study are similar to those from other studies using an HFD/STZ-based model of diabetes (Akın et al., 2020; Nurdiana et al., 2017; Zhang et al., 2017). Notably, treatment of HFD/STZ rats with L-norvaline or the combination of L-norvaline and L-arginine attenuated the increased histological scores, which indicates the protective and preventive effects of LN and LN/LA. In kidney tissues, the STZ and STZ_LN groups showed no obvious differences from one another (Fig. 5, e), but the greater improvement was noticeable in the STZ_LN_LA group. These results may be associated with the possible protective effect of L-norvaline and L-arginine on diabetes-induced tissue damage, mediated by regulation of NOS activity and NO synthesis. NO plays many different roles in the kidney, including controlling renal and glomerular hemodynamics. Its net effect is to promote natriuresis and diuresis, along with renal adaptation to dietary salt intake (Dellamea et al., 2014). Notably, the kidney is an important factor in overall body NO homeostasis. In a diabetic kidney, hyperglycemia, hypertension, and proteinuria are the main insults that cause structural abnormalities. Regulation of NOS is impaired during he development and progression of renal damage that leads to kidney failure (Dellamea et al., 2014), while disturbed NO metabolism is present in diabetes associated with nephropathy (Tessari, 2015). Indeed, all three NOS isoforms have been reported to modulate oxygen consumption, substrate use, hypertrophy, apoptosis, and regenerative potential in various cells through regulating NO synthesis (Akın et al., 2020). As T2DM and hyperglycemia cause structural damage to both the pancreas and the kidney, it is important to maintain NO levels to protect those tissues from the harmful effects of hyperglycemia.

In addition to the histological scores mentioned above, we found pancreas samples from HFD/STZ hyperglycemic rats to exhibit decreases in the areas of islets and blood vessels and in total islet cells relative to the control group (Fig. 6). The proposed treatment model ameliorated these changes, effectively influencing the respective share of tissue occupied by the islets of Langerhans, various components of the stroma, and blood vessels of the pancreas and kidney. Moreover, the LN_LA combination was more effective than LN alone in maintaining islet area and total islet cell count (Fig. 6).

4.6. Summary

It should be noted that the combination of L-norvaline and L-arginine acts effectively but not on all markers. The combination is more effective than L-norvaline alone regarding the quantity of nitrite anions and elevating Langerhans islet cell numbers, and the reduction of total cholesterol, LDL, and MDA (in week 12). A difference in histological scores is visible, but statistically not significant. Further studies on the difference in glucose levels, arginase activity, and histological scores can be achieved by modifying the doses of these compounds or by using another arginase inhibitor. Importantly, our results showed that both treatments (L-norvaline alone and its combination with L-arginine) might also be applied in the context of prediabetes. If recongized early,

prediabetes can be reversed by regulating the L-arginine pathway to restore NO bioavailability. Thus, this proposed model could make a significant contribution to the prevention of diabetes. In summary, our study suggests that combination treatment with L-norvaline and L-arginine could provide a promising therapeutic tool to prevent changes caused by hyperglycemia. This protective effect is based on an increase of NO levels followed by reductions in blood glucose, LDL, and cholesterol levels; decreased lipid peroxidation; and prevention of histopathological changes in the pancreas and kidney (Fig. 7).

5. Limitations of the study

The current work studied the effects of L-norvaline and L-arginine in HFD/STZ-induced hyperglycemic rats. It should be noted that the success rate for inducing T2DM in rats with 30 mg/kg STZ twice-injected is 30–85% (Zhang et al., 2008). In this work, such induction resulted in the formation of stable hyperglycemia (fasting glucose ≥7.8 mmol/L), whereas T2DM requires a value higher than 11.2 mmol/L. To achieve that threshold, it is planned in the next study to implement a higher dose of STZ, 40 mg/kg, specifically intended for inducing T2DM. In addition, it remains necessary to examine the molecular mechanism of action by which L-norvaline and L-arginine enact their roles. Further research is likewise needed to study the quantitative changes in blood insulin and inflammatory cytokines, and to perform tests for insulin resistance and glucose intolerance. Moreover, other staining modalities should be employed to investigate other histological scores and observe in detail the changes in beta cells. In this work, the study was performed on male rats; in the next, it is planned to apply the treatment model in female rats. This will allow us to compare results between and make observations for both sexes. As the combination of L-norvaline and L-arginine has already shown an antihyperglycemic effect, we plan to further combine it with Armenian herbs to obtain higher effectiveness as plant polyphenolic compounds are known to mediate L-arginine transport into cells and enhance nitric oxide production (Harisa et al., 2016).

Conflict of interest

The authors declare that they have no conflicts of interest with the contents of this article.

Authors' contributions

EN has carried out the investigations, and HJ analyzed the data. NA and HJ wrote the manuscript. AG conducted all the the histological experiments. AM and NA corrected and edited the manuscript. All authors read and accepted the final version of the manuscript.

Funding

The work was supported by the Science Committee of MESCS RA, in the frames of Basic support to Research Institute of Biology, Yerevan State University, the research project № 19YR-1F042, 20TTSG-1F004, 21T-1F283 and the research grant biochem-2284 from the Yervant Terzian Armenian National Science and Education Fund (ANSEF) based in New York, USA.

Author statement

Edita Nadiryan has carried out the investigations, and Hayarpi Javrushyan analyzed the data. Nikolay Avtandilyan and Hayarpi Javrushyan wrote the manuscript. Aanna Grigoryan conducted all the histological experiments. Alina Maloyan and Nikolay Avtandilyan corrected and edited the manuscript. All authors read and accepted the final version of the manuscript.

References

2010/63/EU, 2010. Directive 2010/63/EU of the European parliament and of the Council of 22 September 2010 on the protection of animals used for scientific purposes. Off. J. Eur. Union 1–61.

Abdullah, S., Jarrar, Y., Alhawari, H., Abed, E., Zihlif, M., 2020. The influence of endothelial nitric oxide synthase (eNOS) genetic polymorphisms on cholesterol blood levels among type 2 diabetic patients on atorvastatin therapy. Endocr Metab Immune Disord Drug Targets 21, 352–359. https://doi.org/10.2174/1871530320666200621174858.

Adela, R., Nethi, S.K., Bagul, P.K., Barui, A.K., Mattapally, S., Kuncha, M., Patra, C.R., Reddy, P.N.C., Banerjee, S.K., 2015. Hyperglycaemia enhances nitric oxide production in diabetes: a study from South Indian patients. PLoS One 10, 1–17. https://doi.org/10.1371/journal.pone.0125270.

Akın, A.T., Kaymak, E., Öztürk, E., Sayan, M., Karabulut, D., 2020. Histological examination of rat heart tissue with chronic diabetes. Gaziantep Islam Sci. Technol. Univ. 1, 17–22. https://doi.org/10.46871/eams.2020.2.

Al-Rasheed, Nouf M., Al-Rasheed, Nawal M., Hasan, I.H., Al-Amin, M.A., Al-Ajmi, H.N., Mahmoud, A.M., 2016. Sitagliptin attenuates cardiomyopathy by modulating the JAK/STAT signaling pathway in experimental diabetic rats. Drug Des. Dev. Ther. 10, 2095–2107. https://doi.org/10.2147/DDDT.S109287.

Aluko, E.O., Omobowale, T.O., Oyagbemi, A.A., Adejumobi, O.A., Ajibade, T.O., Fasanmade, A.A., 2018. Reduction in nitric oxide bioavailability shifts serum lipid content towards atherogenic lipoprotein in rats. Biomed. Pharmacother. 101, 792–797. https://doi.org/10.1016/j.biopha.2018.03.001.

Assmann, T.S., Brondani, L.A., Bouças, A.P., Rheinheimer, J., de Souza, B.M., Canani, L. H., Bauer, A.C., Crispim, D., 2016. Nitric oxide levels in patients with diabetes mellitus: a systematic review and meta-analysis. Nitric Oxide Biol. Chem. 61, 1–9. https://doi.org/10.1016/j.niox.2016.09.009.

Avtandilyan, N., Javrushyan, H., Petrosyan, G., Trchounian, A., 2018. The involvement of arginase and nitric oxide synthase in breast cancer development: arginase and NO synthase as therapeutic targets in cancer. Biomed. Res. Int. 2018, 1–9. https://doi.org/10.1155/2018/8696923.

Ayub, S.G., Ayub, T., Khan, S.N., Dar, R., Andrabi, K.I., 2011. Reduced nitrate level in individuals with hypertension and diabetes. J. Cardiovasc. Dis. Res. 2, 172–176. https://doi.org/10.4103/0975-3583.85264.

Bender, S.B., Herrick, E.K., Lott, N.D., Klabunde, R.E., 2007. Diet-induced obesity and diabetes reduce coronary responses to nitric oxide due to reduced bioavailability in isolated mouse hearts. Diabetes. Obes. Metab. 9, 688–696. https://doi.org/10.1111/j.1463-1326.2006.00650.x.

Bonavida, B., 2015. Nitric Oxide and Cancer: Pathogenesis and Therapy. Springer International Publishing, Switzerland.

Brodsky, S.V., Morrishow, A.M., Dharia, N., Gross, S.S., Goligorsky, M.S., 2001. Glucose scavenging of nitric oxide. Am. J. Physiol. Ren. Physiol. 280, 480–486. https://doi.org/10.1152/ajprenal.2001.280.3.f480.

Chen, J. Yi, Ye, Z. Xin, Wang, X. Fen, Chang, J., Yang, M. Wen, Zhong, H. Hua, Hong, F. Fang, Yang, S. Long, 2018. Nitric oxide bioavailability dysfunction involves in atherosclerosis. Biomed. Pharmacother. 97, 423–428. https://doi.org/10.1016/j.biopha.2017.10.122.

Chikani, G., Zhu, W., Smart, E.J., 2004. Lipids: potential regulators of nitric oxide generation. Am. J. Physiol. Endocrinol. Metab. 287, 386–389. https://doi.org/10.1152/ajpendo.00106.2004.

Dellamea, B.S., Leitão, C.B., Friedman, R., Canani, L.H., 2014. Nitric oxide system and diabetic nephropathy. Diabetol. Metab. Syndr. 6, 1–6. https://doi.org/10.1186/1758-5996-6-17.

DiNicolantonio, J.J., Lucan, S.C., O'Keefe, J.H., 2016. The evidence for saturated fat and for sugar related to coronary heart disease. Prog. Cardiovasc. Dis. 58, 464–472. https://doi.org/10.1016/j.pcad.2015.11.006.

Förstermann, U., Xia, N., Li, H., 2017. Roles of vascular oxidative stress and nitric oxide in the pathogenesis of atherosclerosis. Circ. Res. 120, 713–735. https://doi.org/10.1161/CIRCRESAHA.116.309326.

Furman, B.L., 2021. Streptozotocin-induced diabetic models in mice and rats. Curr. Protoc. 1, 1–21. https://doi.org/10.1002/cpz1.78.

Galicia-Garcia, U., Benito-Vicente, A., Jebari, S., Larrea-Sebal, A., Siddiqi, H., Uribe, K.B., Ostolaza, H., Martín, C., 2020. Pathophysiology of type 2 diabetes mellitus. Int. J. Mol. Sci. 21, 1–34. https://doi.org/10.3390/ijms21176275.

Gerber, P.A., Rutter, G.A., 2017. The role of oxidative stress and hypoxia in pancreatic beta-cell dysfunction in diabetes mellitus. Antioxid. Redox Signal. 26, 501–518. https://doi.org/10.1089/ars.2016.6755.

Gilinsky, M.A., Polityko, Y.K., Markel, A.L., Latysheva, T.V., Samson, A.O., Polis, B., Naumenko, S.E., 2020. Norvaline reduces blood pressure and induces diuresis in rats with inherited stress-induced arterial hypertension. Biomed. Res. Int. 2020 https://doi.org/10.1155/2020/4935386.

Gori, T., 2020. Exogenous no therapy for the treatment and prevention of atherosclerosis. Int. J. Mol. Sci. 21 https://doi.org/10.3390/ijms21082703.

Guo, X. Xuan, Wang, Y., Wang, K., Ji, B. Ping, Zhou, F., 2018. Stability of a type 2 diabetes rat model induced by high-fat diet feeding with low-dose streptozotocin injection. J Zhejiang Univ Sci B 19, 559–569. https://doi.org/10.1631/jzus.B1700254.

Harisa, G.I., Attia, S.M., Abd Allah, G.M., 2016. Natural cholesterol busters. Cholest. Low. Ther. Drug 1–16. https://doi.org/10.5772/64077.

Hintze, K.J., Benninghoff, A.D., Cho, C.E., Eward, R., 2018. Modeling the western diet for preclinical investigations. Adv. Nutr. 9, 263–271. https://doi.org/10.1093/advances/nmy002.

Hirano, T., 2018. Pathophysiology of diabetic dyslipidemia. J. Atheroscler. Thromb. 25, 771–782. https://doi.org/10.5551/jat.RV17023.

Hoshiyama, M., Li, B., Yao, J., Harada, T., Morioka, T., Oite, T., 2003. Effect of high glucose on nitric oxide production and endothelial nitric oxide synthase protein expression in human glomerular endothelial cells. Nephron Exp. Nephrol. 95 https://doi.org/10.1159/000073673.

Hua, J., Malinski, T., 2019. Variable effects of LDL subclasses of cholesterol on endothelial nitric oxide/peroxynitrite balance – the risks and clinical implications for cardiovascular disease. Int. J. Nanomedicine 14, 8973–8987. https://doi.org/10.2147/IJN.S223524.

Huang, J., Cai, C., Zheng, T., Wu, X., Wang, D., Zhang, K., Xu, B., Yan, R., Gong, H., Zhang, J., Shi, Y., Xu, Z., Zhang, Xue, Zhang, Xuemin, Shang, T., Zhou, J., Guo, X., Zeng, C., Lai, E.Y., Xiao, C., Xiao, C., Chen, J., Wan, S., Liu, W.H., Ke, Y., Cheng, H., Cheng, H., 2020. Endothelial scaffolding protein ENH (enigma homolog protein) promotes PHLPP2 (pleckstrin homology domain and leucine-rich repeat protein phosphatase 2)-mediated dephosphorylation of AKT1 and eNOS (endothelial NO synthase) promoting vascular remodeling. Arterioscler. Thromb. Vasc. Biol. 2, 1705–1721. https://doi.org/10.1161/ATVBAHA.120.314172.

Kashyap, S.R., Lara, A., Zhang, R., Young, M.P., DeFronzo, R.A., 2008. Insulin reduces plasma arginase activity in type 2 diabetic patients. Diabetes Care 31, 134–139. https://doi.org/10.2337/dc07-1198.

Kim, F., Pham, M., Maloney, E., Rizzo, N.O., Morton, G.J., Wisse, B.E., Kirk, E.A., Chait, A., Schwartz, M.W., 2008. Vascular inflammation, insulin resistance, and reduced nitric oxide production precede the onset of peripheral insulin resistance. Arterioscler. Thromb. Vasc. Biol. 28, 1982–1988. https://doi.org/10.1161/ATVBAHA.108.169722.

Konovalova, E.A., Chernomortseva, E.S., 2019. The study of the endothelial protective properties of the L-norvaline combination with mexidol in the simulation of L-NAME-induced NO deficiency. Res. Result Pharmacol. 5, 41–46. https://doi.org/10.3897/RRPHARMACOLOGY.5.38405.

Kövamees, O., Shemyakin, A., Checa, A., Wheelock, C.E., Lundberg, J.O., Östenson, C.G., Pernow, J., 2016. Arginase inhibition improves microvascular endothelial function in patients with type 2 diabetes mellitus. J. Clin. Endocrinol. Metab. 101, 3952–3958. https://doi.org/10.1210/jc.2016-2007.

Krause, M., Rodrigues-Krause, J., O'Hagan, C., De Vito, G., Boreham, C., Susta, D., Newsholme, P., Murphy, C., 2012. Differential nitric oxide levels in the blood and skeletal muscle of type 2 diabetic subjects may be consequence of adiposity: a preliminary study. Metabolism 61, 1528–1537. https://doi.org/10.1016/j.metabol.2012.05.003.

Lee, Y.S., Lee, D., Park, G.S., Ko, S.H., Park, J., Lee, Y.K., Kang, J., 2021. Lactobacillus plantarum HAC01 ameliorates type 2 diabetes in high-fat diet and streptozotocin-induced diabetic mice in association with modulating the gut microbiota. Food Funct. 12, 6363–6373. https://doi.org/10.1039/d1fo00698c.

Lertpatipanpong, P., Lee, J., Kim, I., Eling, T., Oh, S.Y., Seong, J.K., Baek, S.J., 2021. The anti-diabetic effects of NAG-1/GDF15 on HFD/STZ-induced mice. Sci. Rep. 11, 1–13. https://doi.org/10.1038/s41598-021-94581-y.

Li, S., Huang, Q., Zhang, L., Qiao, X., Zhang, Y., Tang, F., Li, Z., 2019. Effect of CAPE-pNO2 against type 2 diabetes mellitus via the AMPK/GLUT4/ GSK3β/PPARα pathway in HFD/STZ-induced diabetic mice. Eur. J. Pharmacol. 853, 1–10. https://doi.org/10.1016/j.ejphar.2019.03.027.

Li, Y., Hou, J. Gang, Liu, Z., Gong, X. Jie, Hu, J. Nan, Wang, Y. Ping, Liu, W. Cong, Lin, X. Hui, Wang, Z., Li, W., 2021. Alleviative effects of 20(R)-Rg3 on HFD/STZ-induced diabetic nephropathy via MAPK/NF-κB signaling pathways in C57BL/6 mice. J. Ethnopharmacol. 267, 113500 https://doi.org/10.1016/j.jep.2020.113500.

Lundberg, J.O., Gladwin, M.T., Weitzberg, E., 2015. Strategies to increase nitric oxide signalling in cardiovascular disease. Nat. Rev. Drug Discov. 14, 623–641. https://doi.org/10.1038/nrd4623.

March, R., 1989. Method Lipoprotein of Tocopherol Fractions Precipitation Determination Using a Heparin-Ca Technique In View of the Delivery of Tocopherol to Effective Sites in Tissues and Cells , Circulating Tocopherol is Believed to be Distributed into Lipoproteins Sinc, pp. 235–242.

Ming, M., Li, X., Fan, X., Yang, D., Li, L., Chen, S., Gu, Q., Le, W., 2009. Retinal pigment epithelial cells secrete neurotrophic factors and synthesize dopamine: possible contribution to therapeutic effects of RPE cell transplantation in Parkinson's disease. J. Transl. Med. 7, 1–9. https://doi.org/10.1186/1479-5876-7-53.

Muronetz, V.I., Medvedeva, M.V., Sevostyanova, I.A., Schmalhausen, E.V., 2021. Modification of glyceraldehyde-3-phosphate dehydrogenase with nitric oxide: role in signal transduction and development of apoptosis. Biomolecules 11. https://doi.org/10.3390/biom11111656.

Napoli, C., de Nigris, F., Williams-Ignarro, S., Pignalosa, O., Sica, V., Ignarro, L.J., 2006. Nitric oxide and atherosclerosis: an update. Nitric Oxide Biol. Chem. 15, 265–279. https://doi.org/10.1016/j.niox.2006.03.011.

Nurdiana, S., Goh, Y.M., Ahmad, H., Dom, S.M., Syimal'ain Azmi, N., Noor Mohamad Zin, N.S., Ebrahimi, M., 2017. Changes in pancreatic histology, insulin secretion and oxidative status in diabetic rats following treatment with Ficus deltoidea and vitexin. BMC Complement. Altern. Med. 17, 1–17. https://doi.org/10.1186/s12906-017-1762-8.

O'Donnell, V.B., Freeman, B.A., 2001. Interactions between nitric oxide and lipid oxidation pathways: implications for vascular disease. Circ. Res. 88, 12–21. https://doi.org/10.1161/01.RES.88.1.12.

Pernow, J., Jung, C., 2013. Arginase as a potential target in the treatment of cardiovascular disease: reversal of arginine steal? Cardiovasc. Res. 98, 334–343. https://doi.org/10.1093/cvr/cvt036.

Petrie, J.R., Guzik, T.J., Touyz, R.M., 2018. Diabetes, hypertension, and cardiovascular disease: clinical insights and vascular mechanisms. Can. J. Cardiol. 34, 575–584. https://doi.org/10.1016/j.cjca.2017.12.005.

Pitocco, D., Zaccardi, F., Di Stasio, E., Romitelli, F., Santini, S.A., Zuppi, C., Ghirlanda, G., 2010. Oxidative stress, nitric oxide, and diabetes. Rev. Diabet. Stud. 7, 15–25. https://doi.org/10.1900/RDS.2010.7.15.

Pokrovskiy, M.V., Korokin, M.V., Tsepeleva, S.A., Pokrovskaya, T.G., Gureev, V.V., Konovalova, E.A., Gudyrev, O.S., Kochkarov, V.I., Korokina, L.V., Dudina, E.N., Babko, A.V., Terehova, E.G., 2011. Arginase inhibitor in the pharmacological correction of endothelial dysfunction. Int. J. Hypertens. 2011 https://doi.org/10.4061/2011/515047.

Polis, B., Srikanth, K.D., Gurevich, V., Gil-Henn, H., Samson, A.O., 2019. L-Norvaline, a new therapeutic agent against Alzheimer's disease. Neural Regen. Res. 14, 1562–1572. https://doi.org/10.4103/1673-5374.255980.

Rafikov, R., Fonseca, F.V., Kumar, S., Pardo, D., Darragh, C., Elms, S., Fulton, D., Black, S.M., 2011. eNOS activation and NO function: structural motifs responsible for the posttranslational control of endothelial nitric oxide synthase activity. J. Endocrinol. 210, 271–284. https://doi.org/10.1530/JOE-11-0083.

Richmond, W., 1992. Analytical reviews in clinical biochemistry: the quantitative analysis of cholesterol. Ann. Clin. Biochem. 29, 577–597. https://doi.org/10.1177/000456329202900601.

Roediger, W.E., Hems, R., Wiggins, D., Gibbons, G.F., 2004. Inhibition of hepatocyte lipogenesis by nitric oxide donor: could nitric oxide regulate lipid synthesis? IUBMB Life 56, 35–40. https://doi.org/10.1080/15216540310001649822.

Salama, A., Asaad, G., Shaheen, A., 2022. Chrysin ameliorates STZ-induced diabetes in rats: possible impact of modulation of TLR4/NF-κβ pathway. Res. Pharm. Sci. 17, 1–11. https://doi.org/10.4103/1735-5362.329921.

Schirmer, S.H., Werner, C.M., Laufs, U., Bhm, M., 2012. Nitric oxide-donating statins: a new concept to boost the lipid-independent effects. Cardiovasc. Res. 94, 395–397. https://doi.org/10.1093/cvr/cvs148.

Schofield, J.D., Liu, Y., Rao-Balakrishna, P., Malik, R.A., Soran, H., 2016. Diabetes dyslipidemia. Diabetes Ther. 7, 203–219. https://doi.org/10.1007/s13300-016-0167-x.

Seneff, S., Lauritzen, A., Davidson, R., Lentz-Marino, L., 2012. Is endothelial nitric oxide synthase a moonlighting protein whose day job is cholesterol sulfate synthesis? Implications for cholesterol transport, diabetes and cardiovascular disease. Entropy 14, 2492–2530. https://doi.org/10.3390/e14122492.

Spormann, H., Sokolowski, A., Letko, G., 1989. Effect of temporary ischemia upon development and histological patterns of acute pancreatitis in the rat. Pathol. Res. Pract. 184, 507–513. https://doi.org/10.1016/S0344-0338(89)80143-8.

Steppan, J., Nyhan, D., Berkowitz, D.E., 2013. Development of novel arginase inhibitors for therapy of endothelial dysfunction. Front. Immunol. 4, 1–6. https://doi.org/10.3389/fimmu.2013.00278.

Tangvarasittichai, S., 2015. Oxidative stress, insulin resistance, dyslipidemia and type 2 diabetes mellitus. World J. Diabetes 6, 456. https://doi.org/10.4239/wjd.v6.i3.456.

Tatsch, E., Bochi, G.V., Piva, S.J., De Carvalho, J.A.M., Kober, H., Torbitz, V.D., Duarte, T., Signor, C., Coelho, A.C., Duarte, M.M.M.F., Montagner, G.F.F.S., Da Cruz, I.B.M., Moresco, R.N., 2012. Association between DNA strand breakage and oxidative, inflammatory and endothelial biomarkers in type 2 diabetes. Mutat. Res. Fundam. Mol. Mech. Mutagen. 732, 16–20. https://doi.org/10.1016/j.mrfmmm.2012.01.004.

Tessari, P., 2015. Nitric oxide in the normal kidney and in patients with diabetic nephropathy. J. Nephrol. 28, 257–268. https://doi.org/10.1007/s40620-014-0136-2.

Tuhin, R.H., Begum, M., Rahman, S., Karim, R., Begum, T., Ahmed, S.U., Mostofa, R., Hossain, A., Abdel-Daim, M., Begum, R., 2017. Wound healing effect of Euphorbia hirta linn. (Euphorbiaceae) in alloxan induced diabetic rats. BMC Complement. Altern. Med. 17, 1–14. https://doi.org/10.1186/s12906-017-1930-x.

Vodovotz, Y., 1996. Modified microassay for serum nitrite and nitrate. Biotechniques 20, 390–394.

Weibel, E.R., Kistler, G.S., Scherle, W.F., 1966. Practical stereological methods for morphometric cytology. J. Cell Biol. 30, 23–38. https://doi.org/10.1083/jcb.30.1.23.

Wu, J., Yan, L.J., 2015. Streptozotocin-induced type 1 diabetes in rodents as a model for studying mitochondrial mechanisms of diabetic β cell glucotoxicity. Diabetes Metab. Syndr. Obes. Targets Ther. 8, 181–188. https://doi.org/10.2147/DMSO.S82272.

Xue, P., Zhao, J., Zheng, A., Li, L., Chen, H., Tu, W., Zhang, N., Yu, Z., Wang, Q., Gu, M., 2019. Chrysophanol alleviates myocardial injury in diabetic db/db mice by regulating the SIRT1/HMGB1/NF-κB signaling pathway. Exp. Ther. Med. 4406–4412. https://doi.org/10.3892/etm.2019.8083.

Yen, C.H., Sun, C.K., Leu, S., Wallace, C.G., Lin, Y.C., Chang, L.T., Chen, Y.L., Tsa, T.H., Kao, Y.H., Shao, P.L., Hsieh, C.Y., Chen, Y.T., Yip, H.K., 2012. Continuing exposure to low-dose nonylphenol aggravates adenine-induced chronic renal dysfunction and role of rosuvastatin therapy. J. Transl. Med. 10 https://doi.org/10.1186/1479-5876-10-147.

Zeb, A., Ullah, F., 2016. A simple spectrophotometric method for the determination of thiobarbituric acid reactive substances in fried fast foods. J. Anal. Methods Chem. 2016 https://doi.org/10.1155/2016/9412767.

Zhang, M., Lv, X.Y., Li, J., Xu, Z.G., Chen, L., 2008. The characterization of high-fat diet and multiple low-dose streptozotocin induced type 2 diabetes rat model. Exp. Diabetes Res. 2008, 704045 https://doi.org/10.1155/2008/704045.

Zhang, C., Li, J., Hu, C., Wang, J., Zhang, J., Ren, Z., Song, X., Jia, L., 2017. Antihyperglycaemic and organic protective effects on pancreas, liver and kidney by polysaccharides from Hericium erinaceus SG-02 in streptozotocin-induced diabetic mice. Sci. Rep. 7, 1–13. https://doi.org/10.1038/s41598-017-11457-w.